JBUON 2017; 22(4): 1061-1067
ISSN: 1107-0625, online ISSN: 2241-6293 • www.jbuon.com
E-mail: editorial_office@jbuon.com

ORIGINAL ARTICLE

Differentiation between progression and pseudoprogression by arterial spin labeling MRI in patients with glioblastoma multiforme

Marija Jovanovic[1], Sandra Radenkovic[2], Tatjana Stosic-Opincal[3], Slobodan Lavrnic[1], Svetlana Gavrilovic[1], Biljana Lazovic-Popovic[3,4], Ivan Soldatovic[3,5], Ruzica Maksimovic[1,3]

[1]Clinical Center of Serbia, Radiology and MRI Center, Belgrade; [2]Department of Radiation Oncology and Diagnostics, Institute of Oncology and Radiology of Serbia, Belgrade; [3]Medical Faculty, University of Belgrade, Dr Subotica 8, Belgrade; [4]University Clinical Hospital Center Zemun, Belgrade; [5]Institute for Medical Statistics and Informatics, Belgrade, Serbia

Summary

Purpose: *To compare arterial spin labeling (ASL) perfusion technique with the clinically established dynamic susceptibility contrast-enhanced (DSC) perfusion weighted-imaging (PWI), and to determine its value in routine MRI evaluation of disease progression in patients with glioblastoma multiforme (GBM).*

Methods: *A prospective intraindividual study was performed in 31 patients with histologically proven GBM who had clinical and/or radiological deterioration after treatment, including surgery, radiotherapy and therapy with temozolomide. Conventional brain protocol with ASL and DSC techniques was performed on 3T MRI unit. Cerebral blood flow (CBF) and cerebral blood volume (CBV) maps were analyzed by means of regions of interest (ROI). Each ROI average value was normalized to the contralateral normal brain parenchyma ROI value. Neuroradiologists analyzed CBF and CBV maps separately, and classified patients into progression or pseudoprogression group. Radiological diagnosis was confirmed by clinical-radiological follow-up for at least three months after patient deterioration.*

Results: *High linear correlation existed between DSC-PWI and ASL in the tumor ROI (r=0.733; p<0.001). 92% of ASL CBF maps were informative. ASL detected all lesions as well as DSC MRI. Both techniques provided perfusion values closely correlated.*

Conclusion: *ASL allows distinction between GBM progression and pseudoprogression, and it can be used as reliable alternative to DSC-PWI.*

Key words: *ASL, DSC, glioblastoma, perfusion, pseudoprogression*

Introduction

Although surgical resection followed by radiotherapy and different modalities of chemotherapy have increased the overall survival of patients with GBM [1-3], they have hampered neuroradiological diagnostic.

If increasing size and postcontrast enhancement of the existing lesion and/or the lesion's number is detected on postsurgical control conventional brain MRI with contrast administration (cMRI), the diagnosis of recurrent GBM (progression) or treatment effects (pseudoprogression) is made [4-6]. Both entities appear on MRI as contrast enhancing lesions with edema and mass effect [5-7]. Unlike GBM progression, pseudoprogression is an inflammatory reaction of brain tissue with increased permeability of normal vascular network and edema after radiochemotherapy [6,7]. Accordingly, GBM progression demands reoperation or different oncological therapy, while pseudoprogression requires follow-up with or

Correspondence to: Sandra Radenkovic, MD, PhD. Department of Radiation Oncology and Diagnostics, Institute of Oncology and Radiology of Serbia, Pasterova 14, 11000 Belgrade, Serbia.
Tel: +381 642060648, Fax: +381 112685300, E-mail: stankovics@ncrc.ac.rs
Received: 27/03/2017; Accepted: 12/04/2017

without symptomatic therapy. Wrong diagnosis consequently influences the patient's quality of life, survival and outcome [8].

McDonald and The Response Assessment in Neuro-Oncology (RANO) working group based the therapy response criteria of malignant gliomas on clinical parameters and cMRI findings [9]. However, contrast enhancement of the lesions reflects rather disruption of blood-brain barrier (BBB), emphasized by corticosteroids, radio- and chemotherapy, than the presence and degree of neovascularity [5,6,10-12]. Therefore, clear differentiation between therapy sequelae and recurrent GBM cannot be achieved with cMRI sequences alone.

Tissues microvascular hemodynamic elucidates PWI techniques. DSC is mostly used and clinically accepted PWI, which allows the measurement of the CBV and CBF. Although numerous studies have shown the utility of DSC in the differentiation of tumor recurrence from treatment effects [13-17], there are several disadvantages of using intravascular contrast bolus in the oncological patients' follow-up [7].

In order to avoid repeated contrast injections, as well as to analyze the absolute perfusion values, the clinical use of ASL technique is increasing.

The purpose of this study was to compare ASL and DSC perfusion techniques, and to estimate the value of ASL in the differentiation of progression from pseudoprogression in patients with GBM. For the time being, there is only one published article that analyzed particularly the value of ASL in the differentiation of GBM progression and pseudoprogression, but using the qualitative analysis of CBF-ASL parameter [18]. To the best of our knowledge, this is the first article that specifically analyzed the value of ASL in the differentiation of GBM progression from pseudoprogression using two-dimensional (2D) pseudocontinuous ASL (PASL) perfusion technique and normalizing the obtained quantitative CBF-ASL values of brain lesions with contralateral normal-appearing white or gray matter.

Methods

Study population

This prospective study was approved by the institutional Ethics Committee. The intraindividual study was performed in 31 patients with histologically proven GBM, who had clinical and/or radiological deterioration during postsurgical conformal radiotherapy and concomitant or adjuvant oral therapy with temozolomide. All patients received radiation therapy with total dose of 60 Gy given in 30 fractions during 6 weeks fractionated in 2 Gy per day. Concomitant oral application of temozolomide included dose of 75 mg/m^2/day, followed by six cycles of 150 mg/m^2/day for 5 days every 28 days.

MRI protocol

Control brain MRI was performed on a 3 Tesla MRI unit (Skyra, Siemens, Germany) with a standard eight-channel transmit/receive head coil. The protocol included axial and sagittal T2-weighted imaging, axial T1-weighted imaging, coronal fluid attenuated inversion recovery sequence, diffusion-weighted imaging, and multiplanar reconstructed transverse, coronal and sagittal imaging with a three-dimensional (3D) magnetization-prepared rapid acquisition gradient-echo (MPRAGE) sequence after contrast application.

ASL technique was performed before contrast medium administration as 2D pseudocontinuous ASL method (PICORE Q2T) with imaging parameters: repetition time (TR) 2500 ms; echo time (TE) 12 ms; acquisition matrix 64x64; field of view (FOV) 256 mm; slice thickness 8 mm; interslice gap 25%; inversion time (IT) 1800 ms; post label delay 0 ms; number of measurements 91; acquisition voxel size 4x4x8 mm; and relative signal-to-noise ratio (SNR) 1.

The DSC PWI was performed with a single-shot gradient-echo planar imaging (EPI) sequence with the following parameters: TR 1950 ms, TE 30 ms; flip angle (FA) 90^o; acquisition matrix 128x128; FOV 220 mm; slice thickness 4 mm; interslice gap 10%; and relative SNR 1. The DSC PWI technique was applied during the intravenous administration of 0.2 mmol/kg of gadopentetate dimeglumine (Magnevist; Bayer Schering Pharma AG, Berlin, Germany) at a flow rate of 5 mL/s with an MRI compatible power injector (Spectris; Medrad, Germany) through a 20-gauge peripheral angiocatheter. The bolus of contrast material was followed by a 20 mL bolus of saline administered at the same injection rate.

Image analysis

Image processing was performed using commercially available software (Syngo Via, Siemens, Germany). Two neuroradiologist (25 and 7 years of experience, respectively), blinded to the clinical findings, analyzed three imaging sets within an interval of at least four weeks to avoid intraobserver bias. Imaging sets were: 1) cMRI with ASL; 2) cMRI with DSC PWI; 3) cMRI with ASL and DSC PWI. The lesions were classified as tumor progression or as treatment effects , or as pseudoprogression. In case of disagreement, the final MRI diagnosis was made by consensus.

A single ROI (area 0.20-0.50 cm^2) was manually drawn in the lesion area with the most intense contrast-enhancement, and then transferred to corresponding location on CBF-ASL and CBV-DSC maps. The ROI was also applied in the adequate contralateral normal-appearing brain tissue. Cystic, necrotic or hemorrhagic parts of the lesion, adjacent bone, air and blood vessels, were excluded from the ROI. For each ROI, the mean CBF and CBV values were measured. Normalized CBF (nCBF) and CBV (nCBF) values were calculated as $CBF_{lesion}/CBF_{normal\text{-}appiring\ tissue}$ (CBFl/CBFn) ratio

and $CBV_{lesion}/CBV_{normal\text{-}appiring\ tissue}$ (CBVl/CBVn) ratio, respectively.

Final diagnosis

Radiological diagnosis was confirmed by clinical-radiological follow-up for at least three months after patient deterioration. Regular neurological examination and Karnofsky performance status evaluation were performed by neurosurgeons. The patient condition was defined as progression, if clinical or MRI findings (presence of progressively enhancing lesions) indicated change of treatment protocol within three months after initial deterioration. A diagnosis of pseudoprogression was made in cases without treatment change, based on patient clinical condition and follow-up cMRI (presence of non-progressively enhancing lesions on the scan within three months after initial cMRI with ASL and DSC PWI). Clinical and control cMRI data were compared to ASL and DSC PWI findings.

Statistics

Data are presented as numbers (%) or mean values (± standard deviation). Comparison between two measurements was performed using Wilcoxon Singed Ranks test, while Mann-Whitney U test was used for group comparisons. ROC analysis was used to assess cut-off values of CBV and CBF for tumor presence. Correlation analysis was used to evaluate agreement between CBV and CBF. All data analyses were performed using SPSS 20 (IBM corp.). All p values less than 0.05 were considered statistically significant.

Results

The study was performed in 21 men and 10 women with GBM, with a mean age of 49±13.84 years (range of 21-73). Twenty patients (64.52%) were subsequently classified as having GBM progression and 11 (35.48%) as having GBM pseudoprogression. Fifteen patients (48.38%) showed clinical deterioration, while 16 (51.61%) were clinically stable. Disease progression was confirmed by clinical exacerbation in 15 patients (75%), and by presence of progressive enhancing lesions on control cMRI in 5 (25%). Pseudoprogression diagnosis was confirmed by clinical stable status and absence of progressively enhancing lesions on control cMRI in 11 patients (100%).

Representative images of patients with GBM progression and pseudoprogresion are presented in Figures 1 and 2, respectively.

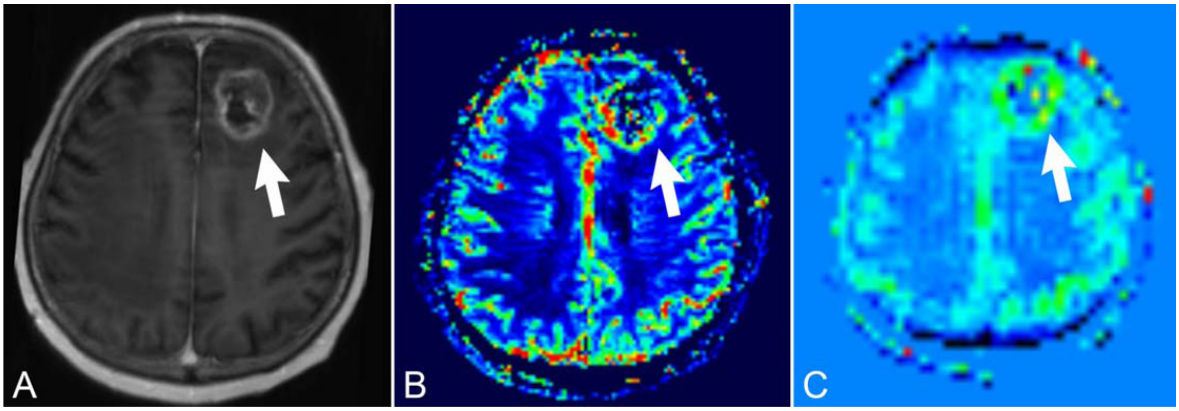

Figure 1. GBM progression in a 57-year-old man. **(A)** Axial postcontrast T1-weighted image shows necrotic contrast-enhancing lesion in the left frontal lobe (arrow). Axial **(B)** DSC and **(C)** ASL perfusion maps show increased signal intensity in the corresponding area with the contrast enhancement (arrows).

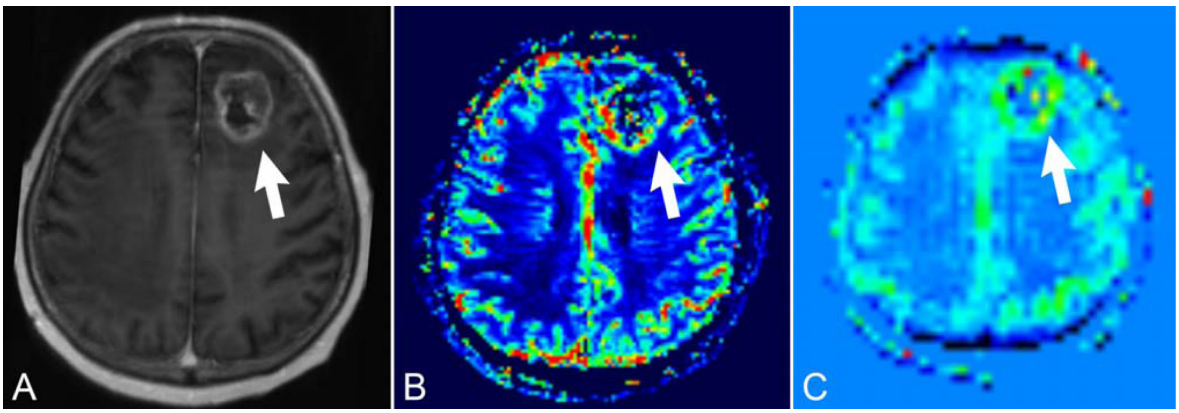

Figure 2. GBM pseudoprogression in a 55-year-old man. **(A)** Axial postcontrast T1-weighted image shows necrotic contrast-enhancing lesion in the left frontal lobe (arrow). Axial **(B)** DSC and **(C)** ASL perfusion maps show absence of increased signal intensity in the corresponding area with the contrast enhacement (arrows).

All of the quantitative imaging parameters showed significant differences between GBM progression and pseudoprogression.

As shown in Figure 3, the linear correlation analysis revealed that there was a close correlation between nCBF-ASL and nCBV-DSC values, with r=0.733, which was statistically different with p<0.001. Using ROC curve, the cut off value 2.89 for CBV had 100% sensitivity and 100% specificity (AUC=1,000; p<0.001) in determining tumor presence. Similar, CBF value of 0.995 has 100% sensitivity and 73.7% specificity, and value 1.02 had 92.3% sensitivity and 92.9% specificity (AUC=0.967; p<0.001).

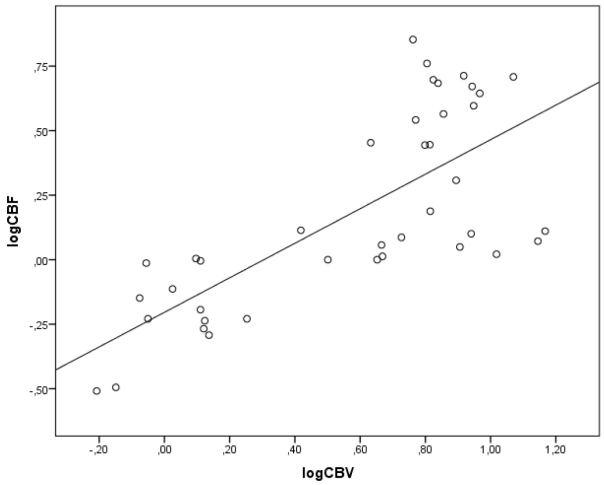

Figure 3. Scatterplot showing n-CBF-ASL and nCBV-DSC values in all patients with GBM.

Discussion

In this study we evaluated the potential of the ASL perfusion technique to be integrated in the routine cMRI protocol for differentiating GBM progression and pseudoprogression. We compared the application of ASL and DSC PWI in patients with GBM who had clinical and/or radiological deterioration during the posttreatment period. Our results demonstrated that there is a high correlation between the ASL and DSC methods, so that ASL has the ability to differentiate tumor recurrence from treatment effects. Our results show that nCBF-ASL and nCBV-DSC quantitative values were significantly higher in patients with GBM progression, than in those with GBM pseudoprogression.

In the DSC, the important factors are the injection rate of contrast agent, quality of the venous access and patient hemodynamics, which are commonly disrupted in oncological patients. Also, contrast agent extravasation from the pathologically changed blood vessels represents important limitation, since it leads to the underestimation the CBV values. However, DSC has several advantages: better SNR, shorter scan time, ease of use, and higher commercial availability [6,19].

Unlike DSC, ASL perfusion technique examines the brain perfusion with endogenous intravascular tracer - hydrogen nuclei of the blood water, and allows the measurement of absolute CBF values of brain tissue. In ASL, protons are "labeled" in the region just below the brain ROI. After a period of time (inversion time, IT), the tagged blood reaches the brain parenchyma, and the imaging in the labeled and control unlabeled state is applied. The magnetization difference between two imaging sets is proportional to the amount of the arterial blood delivered to the ROI. There are two main types of ASL technique – pseudocontinuous (PASL) and continuous (CASL). We performed 2D PASL technique, where the short RF pulse is applied, and the signal acquisition is carried out after a short IT. The ASL signal depends on parameters such as flow rate, T1 relaxation time of the blood and tissue, and transit time of labeled arterial blood from the tagging region to the imaging plane. Since the transit time through the capillary bed of the labeled arterial water is considerably longer than T1 decay, contrast agent extravasation does not influence ASL signal intensity. Therefore, ASL is a non-invasive, repeatable technique, especially suitable in patients who cannot tolerate a contrast bolus injection. Disadvantages of ASL include low SNR and propensity to motion and susceptibility artifacts [19-21].

A number of previous studies have used CBV-DSC and CBF-ASL value for the evaluation of brain tumor perfusion [12,22-26], but only a few previous studies have analyzed CBF-ASL parameter in the differentiation of glioma recurrence from treatment effects [18,27-31].

The nCBV-DSC values obtained in our study are similar with those published in other relevant studies, while the nCBF-ASL values are at lower level in our study compared to other published studies. Previous studies have shown that nCBF-ASL values can differentiate between tumor recurrence and treatment effects, but with different cut-off values. Choi et al. concluded that ASL values with odds ratio of 4.73 could significantly differentiate between GBM progression and pseudoprogression, but they analyzed the perfusion signal qualitatively, comparing it with white and gray matter and blood vessels [18]. Our study included quantitative ASL perfusion values, as more objective ones.

Unlike homogeneous patient group in Choi et al, and in our study, most of these studies included

patients with different glioma grades [18,27-31]. Ozsunar et al. observed patients with different high-grade gliomas who were previously treated only with surgery and proton-beam therapy [27]. Jarnum et al. calculated high nCBF values (4.86) comparing groups of gliomas and non-gliomas with postreatment effects [28]. In the study of Wang et al. CBF parameters were analyzed in patients with high-grade and low-grade gliomas before and after radiotherapy [29]. Nyberg et al. have found that nCBF value of 3.37 can distinguish recurrent tumor from radiation necrosis, but they analyzed different high-grade gliomas [30]. Kim et al. analyzed only patients with GBM progression, and correlated the CBF values and O6-methylguanine DNA methyltransferase promoter methylation status, but in second round of low-dose temozolomide application [31].

In our study group we have calculated CBF values using 2D PASL at 3T MRI, and normalized obtained values with adequate contralateral normal-appearing brain tissue (white or gray matter), in order to reduce the age-dependent variability and perfusion variations between gray and white matter.

The difference in the obtained ASL values among the different studies may be not only because different tumors and their treatment effects were analyzed, but because different ASL techniques and different approaches for perfusion measurement were applied. Ye et al. obtained higher nCBF value both in recurrent tumor (4.45) and in treatment effects (1.22), but they analyzed patients with primary gliomas after radio- and chemotherapy with temozolomide using 3D PASL method and compared the lesions only with contralateral normal white matter [32].

As mentioned above, the low value of the IT in ASL can lead to apparent hypoperfusion of brain tissue [19]. The time needed for protons to cross the gap between the labeling zone and the ROI will differ according to the velocity of the blood and the labeled bolus. The lifespan of labeled protons is limited, while the labeled blood bolus returns to equilibrium depending on the T1 time constant of the blood. Also, in the presence of mass effect of expansive lesions and radiation effects, normal-appearing contralateral brain tissue may have higher water content and be affected by demyelination, which leads to underestimation of the perfusion values [28]. All these conclusions may explain the results of the present study.

Similar to other studies, we used the ROI analysis of perfusion maps as acceptable routine performed by the same radiologists for all measurements, thus minimizing user dependency. Another approach in the evaluation of PWI maps is histogram analyses with higher interobserver agreement, sensitivity and negative predictive value, compared to ROI method [28]. Histogram analysis has not been yet used in the analysis of CBF-ASL maps in the differentiation of GBM progression from pseudoprogression, and may be a new field of research.

The present study has several limitations. Firstly, the study group was rather small. Secondly, the analysis included only the most enhanced lesions, although it is known that GBM infiltration also persists in non-enhancing edema. Finally, 2D PASL technique was used, which may be responsible for lower nCBF values.

The lack of consistency in methodology and the results may be a barrier for the clinical acceptance of ASL. Optimal imaging and reduction of artifacts may be the solution for the diagnostic accuracy of ASL perfusion technique. In further studies calculation of PWI parameters should be correlated with the lesion location in the brain, since it is known that anterior and posterior watershed areas of the brain tissue have prolonged transit time of contrast agent, and frequently appear more hypoperfused [19].

This study has shown that ASL may be integrated in the routine MRI protocol as an alternative to DSC PWI, in the differentiation of GBM pseudoprogression and progression. Although, ASL technique is more sensitive on motion and susceptibility artefacts, reduction of the known technical failures with a more frequent use of ASL would be desirable, especially in the follow-up examinations to avoid repeated contrast injections.

Conflict of interests

The authors declare no confict of interests.

References

1. Peponi E, Tourkantonis I, Tasiou I, Pavlidis N, Pentheroudakis G, Tsekeris P. Prognostic factors in glioblastoma patients managed with radiotherapy combined with temozolomide. JBUON 2014;19:718-23.
2. Aldea MD, Petrushev B, Soritau O et al. Metformin plus sorafenib highly impacts temozolomide resistant glioblastoma stem-like cells. JBUON 2014; 19:502-11.

3. Baritchii A, Jurj A, Soritau O et al. Sensitizer drugs for the treatment of temozolomide-resistant glioblastoma. JBUON 2016;21:199-207.
4. Brandsma D, van den Bent MJ. Pseudoprogression and pseudoresponse in the treatment of gliomas. Curr Opin Neurol 2009;22:633-8.
5. Pruzincová L, Steno J, Srbecký M et al. MR imaging of late radiation therapy- and chemotherapy-induced injury: a pictorial essay. Eur Radiol 2009;19:2716727.
6. Verma N, Cowperthwaite MC, Burnett MG, Markey MK. Differentiating tumor recurrence from treatment necrosis: a review of neurooncologic imaging strategies. Neuro-Oncology 2013;15:515-34.
7. Hygino da Cruz Jr LC, Rodriguez I, Domingues RC, Gasparetto EL, Sorensen AG. Pseudoprogression and Pseudoresponse: Imaging Challenges in the Assessment of Posttreatment Glioma. Am J Neuroradiol 2011;32:1978-85.
8. Young RM, Jamshidi A, Davis G, Sherman JH. Current trends in the surgical management and treatment of adult glioblastoma. Ann Transl Med 2015;3:121.
9. Vogelbaum MA, Jost S, Aghi MK et al. Application of Novel Response/Progression Measures for Surgically Delivered Therapies for Gliomas: Response Assessment in Neuro-Oncology (RANO) Working Group. Neurosurgery 2012;70:234-43.
10. Behin A, Hoang-Xuan K, Carpentier AF, Delattre JY. Primary brain tumours in adults. Lancet 2003;361:323-31.
11. Fang Zhang, Chun-Lei Xu, Chun-Mei Liu. Drug delivery strategies to enhance the permeability of the blood–brain barrier for treatment of glioma. Drug Des Devel Ther 2015;9:2089-100.
12. Warmuth C, Gunther M, Zimmer C. Quantification of Blood Flow in Brain Tumors: Comparison of Arterial Spin Labeling and Dynamic Susceptibility-weighted Contrast-enhanced MR Imaging. Radiology 2003;228:523-32.
13. Barajas RF, Jr, Chang JS, Segal MR et al. Differentiation of recurrent glioblastoma multiforme from radiation necrosis after external beam radiation therapy with dynamic susceptibility-weighted contrast-enhanced perfusion MR imaging. Radiology 2009;253:486-96.
14. Hu LS, Baxter LC, Smith KA et al. Relative cerebral blood volume values to differentiate high-grade glioma recurrence from posttreatment radiation effect: Direct correlation between image-guided tissue histopathology and localized dynamic susceptibility-weighted contrast-enhanced perfusion MR imaging measurements. Am J Neuroradiol 2009;30:552-8.
15. Gahramanov S, Muldoon LL, Varallyay CG et al. Pseudoprogression of glioblastoma after chemo- and radiation therapy: diagnosis by using dynamic susceptibility-weighted contrast-enhanced perfusion MR imaging with ferumoxytol versus gadoteridol and correlation with survival. Radiology 2013;266:842-52.
16. Song YS, Choi SH, Park CK et al. True Progression versus Pseudoprogression in the Treatment of Glioblastomas: A Comparison Study of Normalized Cerebral Blood Volume and Apparent Diffusion Coefficient by Histogram Analysis. Korean J Radiol 2013; 14:662-72.
17. Young RJ, Gupta A, Shah AD et al. MRI perfusion in determining pseudoprogression in patients with glioblastoma. Clin Imaging 2013;37:41-9.
18. Choi YJ, Kim HS, Jahng GH, Kim SJ, Suh DC. Pseudoprogression in patients with glioblastoma: added value of arterial spin labeling to dynamic susceptibility contrast perfusion MR imaging. Acta Radiologica 2013;54:448-54.
19. Pollock JM, Tan H, Kraft RA, Whitlow CT, Burdette JH, Maldjian JA. Arterial Spin Labeled MRI Perfusion Imaging: Clinical Applications. Magn Reson Imaging Clin N Am 2009;17:315-38.
20. Detre JA, Wang J, Wang Z et al. Arterial spin-labeled perfusion MRI in basic and clinical neuroscience. Curr Opin Neurol 2009;22:348-55.
21. Grade M, Hernandez Tamames JA, Pizzini FB, Achten E, Golay X, Smits M. A neuroradiologist's guide to arterial spin labeling MRI in clinical practice. Neuroradiology 2015;57:1181-202.
22. Knutsson L, Van Westenc D, Petersend ET et al. Absolute quantification of cerebral blood flow: correlation between dynamic susceptibility contrast MRI and model-free arterial spin labeling. Magn Res Imaging 2010;28:1-7.
23. Lehmann P, Monet P, de Marco G et al. A comparative study of perfusion measurement in brain tumours at 3 Tesla MR: Arterial spin labeling versus dynamic susceptibility contrast-enhanced MRI. Eur Neurol 2010;64:21-6.
24. Van Westen D, Petersen ET, Wirestam R et al. Correlation between arterial blood volume obtained by arterial spin labelling and cerebral blood volume in intracranial tumours. MAGMA 2011;24:211-23.
25. Thomsen H, Steffensen E, Larsson E-M. Perfusion MRI (dynamic susceptibility contrast imaging) with different measurement approaches for the evaluation of blood flow and blood volume in human gliomas. Acta Radiologica 2012;53:95-101.
26. Roy B, Awasthi R, Bindal A et al. Comparative Evaluation of 3-Dimensional Pseudocontinuous Arterial Spin Labeling With Dynamic Contrast-Enhanced Perfusion Magnetic Resonance Imaging in Grading of Human Glioma. J Comput Assist Tomogr 2013;37:321-6.
27. Ozsunar Y, Mullins ME, Kwong K et al. Glioma recurrence versus radiation necrosis? A pilot comparison of arterial spin-labeled, dynamic susceptibility contrast enhanced MRI, and FDG-PET imaging. Acad Radiol 2010;17:282-90.
28. Järnum H, Steffensen EG, Knutsson L et al. Perfusion MRI of brain tumours: a comparative study of pseudo-continuous arterial spin labelling and dynamic susceptibility contrast imaging. Neuroradiology 2010;52:307-17.
29. Wang P, Li J, Diao Q et al. Assessment of glioma response to radiotherapy using 3D pulsed-continuous arterial spin labeling and 3D segmented volume. Eur J Radiol 2016;85:1987-92.
30. Nyberg E, Honce J, Kleinschmidt-DeMasters BK, Shukri B, Kreidler S, Nagae L. Arterial spin labeling: Pathologically proven superiority over conventional MRI for detection of high-grade glioma progression after treatment. Neuroradiol J 2016;29:377-83.

31. Kim C, Kim HS, Shim WH, Choi CG, Kim SJ, Kim JH. Recurrent Glioblastoma: Combination of High Cerebral Blood Flow with MGMT Promoter Methylation Is Associated with Benefit from Low-Dose Temozolomide Rechallenge at First Recurrence. Radiology 2017;282:212-21.
32. Jing YE, Santosh Kumar Bhagat, Hongomei LI et al. Differentiation between recurrent gliomas and radiation necrosis using arterial spin labeling perfusion imaging. Exp Ther Med 2016;11:2432-6.